Extension of classical viscoelastic models in large deformation to anisotropy and stress softening

Marie Rebouah, Grégory Chagnon

Extension of classical viscoelastic models in large deformation to anisotropy and stress softening

M. Rebouah, G. Chagnon*

Université de Grenoble / CNRS / TIMC-IMAG UMR 5525, Grenoble, F-38041, France.

Abstract

In this paper, an extension of two classical viscoelastic models adapted in large deformation for incompressible rubber like materials or soft tissues is proposed. These models are built by using a three dimensional homogeneization by means of a sphere unit approach. Thus several comparisons between classical formulations and homogeneization on a sphere unit formulation is proposed. An adaptation of those models to describe anisotropy is proposed. Finally an extension of those models to take into account stress softening is described.

Key words: Viscoelasticity . Constitutive equation . Sphere unit model . Anisotropy . Stress-softening

1. Introduction

Rubber like materials are remarkable materials, by means of their capacity to endure large deformations and cyclic loadings. Despite many publications, the prediction of their mechanical behavior is still an open issue. Since last decades, it is well known that soft tissues present a similar behavior to rubber like materials. The main difference is that most of the soft tissues present also an initial anisotropy. Both materials present many non linear phenomena as Mullins Effect (Mullins (1969); Beatty and Krishnaswamy (2000); Diani *et al.* (2006); Vande Geest *et al.* (2006); Natali *et al.* (2009)), permanent set (Dorfmann and Ogden (2004); Peña *et al.* (2011)), hysteresis (Lion (1996); Peña *et al.* (2009)) and time dependent behavior (Christensen (1982); Wineman and Rajagopal (2000); Holzapfel and Simo (1996)). Mullins effect and permanent set are classically taken into account for quasi static behaviors, where the influence of the strain rate is neglected. At the opposite, the time dependency is treated independently without taking into account the stress softening in many studies.
Nevertheless for the most of rubber like materials the modeling depends mainly on the strain rate, and the response varies from purely rubber like material to glassy polymer (Yi *et al.* (2006); Sarva *et al.* (2007)). Soft tissues present also a strain rate dependency. Models were developed to take into account the viscoelasticity of soft tissues and the initial anisotropy due to their structure, see for example (Fung (1993); Miller and Chinzei (1997); Pioletti and Rakotomanana (2000); Miller (2000); Limbert *et al.* (2004); Taylor *et al.* (2009)).

*Corresponding author
Email address: gregory.chagnon@imag.fr (G. Chagnon)

The viscoelasticity in large deformations is classically described according to two different theories. The first theory is the one developed by Green and Rivlin (1957) and Coleman and Noll (1961) by using the principle of Boltzmann superposition. Indeed Green and Rivlin (1957) introduced and supposed that relaxation functions depend only on the time and Coleman and Noll (1961) considered that these functions depend on time and on the actual state of deformation. These models are expressed in term of convolution integrals and were readapted by Berstein *et al.* (1963) and Zapas and Craft (1965) to finally be known as K-BKZ model for fluids. Later, Ogden (1972) and Christensen (1980) developed the extensions of Green and Rivlin (1957) at the first order for the solids. All these models are not numerically implemented except for fluid mechanics, i.e. the K-BKZ model.
The second theory was developed by Green and Tobolsky (1946) by means of differential models with internal variables. The viscoelasticity is classically build up for uniaxial formulations with springs and dashpots and generalized to tensorial formulation. The two standard models used are those of Zenner and Kelvin-Voigt. The readaptation of the differential models, initially proposed by Green and Tobolsky (1946), was stimulated 40 years later by the work of Lubliner (1985). This model is based on the decomposition of the deformation gradient into an elastic part and an inelastic one. Later several authors (Simo, 1987; Govindjee and Simo, 1992b; Holzapfel and Simo, 1996; Lion, 1996; Kaliske and Rothert, 1998) proposed to separate the response of the material as the sum of an elastic and an inelastic stress, thus the internal variable is of "stress" type. Simo (1987) model is equivalent to the K-BKZ model as proved by Reese and Wriggers (1997), and was implemented in a finite element code. More recently, Bergstrom and Boyce (1998) developed also a non linear evolution law for a stress internal variable, this model is today one of the most used. In the same way, Miehe and Göktepe (2005) were the first to proposed a micro-spherical approach to take into account the time dependent viscous effects and the stress softening for initially isotropic materials. The model proposed by Diani *et al.* (2006) presents also a micro sphere unit representation to take into account the viscoelasticity and the stress softening includind the induced anisotropy by the Mullins effect. Other micro mechanics based model were developed in the last decades to take into accont non linear effects and proposed differents way for three dimensional homogeneization (Govindjee and Simo, 1991, 1992b; Rajagopal and Wineman, 1992; De Tommasi *et al.*, 2006, 2010)
The objective of this paper is to compare a classical and a three dimensionnal homogeneization by a sphere unit formulation of two models recently studied by Petiteau *et al.* (2012). Thus, a Convolution Integral Model (CIM) and a Internal Variable Model (IVM) are used in this paper. The IVM used is the one proposed by Huber and Tsakmakis (2000), and CIM is an adaptation of Berstein *et al.* (1963) proposed by Petiteau *et al.* (2012).
First, a presentation of the both classical models is made in the section 2. Then, the sphere unit formulation of these models is developed in section 3. A comparison between classical and sphere unit formulation is proposed in section 4 for different loadings. Then by means of the sphere unit formulation some extensions to turn the modeling anisotropic are proposed. The influence of several parameters are highlighted for different loadings states and for both models in section 5. Finally, stress softening is added in the viscoelastic spherical approach.

2. Presentation of the models

The two viscoelastic isotropic models used in this paper are those used by Petiteau *et al.* (2012). The first one is an IVM deduced from the theory of Green and Rivlin (1957) and the second is

a CIM deduced from the theory of Green and Tobolsky (1946). These two models are quickly recalled in this section, in the incompressible framework.

2.1. Internal Variable Model

The simplest IVM for viscoelasticity was derived by Huber and Tsakmakis (2000) and is represented by a Zenner model. This model is based on the decomposition of the deformation gradient $\mathbf{F}$ between an elastic part $\mathbf{F_e}$, which represents the deformation gradient of a spring and an inelastic part $\mathbf{F_i}$, which represents the deformation gradient of a dashpot as illustrated in Fig.1. Thus, the deformation gradient $\mathbf{F}$ can be expressed as

$$\mathbf{F} = \mathbf{F_e}\mathbf{F_i} \tag{1}$$

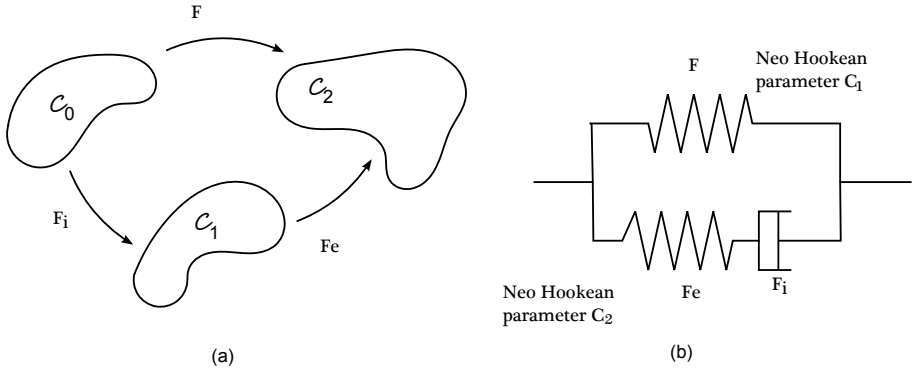

Figure 1: Representation of the different configurations by using a strain type internal variable (a) and the rheological representation of the components (b)

Classically it is considered, that there is no rotation in $\mathbf{F_i}$ and thus the rotation is only in the elastic part $\mathbf{F_e}$. This permits to keep unique the elastic-inelastic decomposition. Furthermore it is assumed that the material is incompressible, thus each deformation is defined as $\det \mathbf{F_e} = 1$ and $\det \mathbf{F_i} = 1$. The strain enery density associated to the rheological representation is defined by:

$$\phi(\mathbf{F_e}, \mathbf{F_i}) = \phi_1(\mathbf{F_e}) + \phi_2(\mathbf{F_i}) \tag{2}$$

where ϕ_1 represents the strain energy density between the initial C_0 and the intermediary C_1 configuration and ϕ_2 the strain energy density between the intermediary C_1 and final C_2 configuration. According to the Second Principle of Thermodynamics

$$\mathcal{D}_{int} = \boldsymbol{\sigma} : \mathbf{D} - \dot{\phi} \geq 0 \tag{3}$$

where $\mathcal{D}_{int}$ is the internal dissipation and $\mathbf{D}$ is the rate of deformation tensor. After some algebric manipulations described in Huber and Tsakmakis (2000) and Petiteau *et al.* (2012), the second principle can be rewritten as

$$\left(\boldsymbol{\sigma} - 2\frac{\partial \phi_1}{\partial \mathbf{B}}\mathbf{B} - 2\frac{\partial \phi_2}{\partial \mathbf{B_e}}\mathbf{B_e}\right) : \mathbf{D} + 2\mathbf{F}^T\frac{\partial \phi_2}{\partial \mathbf{B_e}}\mathbf{F_e} : \mathbf{D}_i \geq 0 \tag{4}$$

where $\mathbf{D}_i$ is the inelastic strain rate tensor defined as $\mathbf{D}_i = 1/2(\mathbf{L}_i + \mathbf{L}_i^T)$ and $\mathbf{L}_i = \dot{\mathbf{F}}_i\mathbf{F}_i^{-1}$ the velocity gradient. $\mathbf{B}$ is the left Cauchy Green tensor (defined as $\mathbf{B} = \mathbf{F}\mathbf{F}^T$) associated to the global deformation and $\mathbf{B_e}$ is the left Cauchy Green tensor (defined as $\mathbf{B_e} = \mathbf{F_e}{\mathbf{F_e}}^T$) associated to the elastic deformation. According to the procedure described by Coleman and Noll (1963) for deformation processes, the incompressibility constraint and to Petiteau *et al.* (2012) who defined a Neo Hookean strain energy (Treloar, 1943) for each spring of the rheological model, it is deduced from Eq.(4) that the Cauchy stress can be described as:

$$\boldsymbol{\sigma} = -p\mathbf{I} + 2C_1\mathbf{B} + 2C_2\mathbf{B_e} \tag{5}$$

and the dissipation

$$2\mathbf{F}^T\frac{\partial\phi_{\mathbf{2}}}{\partial\mathbf{B_e}}\mathbf{F_e} : \mathbf{D}_i \geq 0 \tag{6}$$

where C_1 the material parameter of the Neo Hookean model associated to the global deformation and C_2 is the material parameter of the Neo Hookean model of the elastic part. It is quickly recalled that a Neo Hookean model is defined as $W = C_1(I_1 - 3)$, where I_1 is the first strain invariant. It is deduced as in Petiteau *et al.* (2012) that for uniaxial extension in the direction $\vec{x}$ the first component of the stress tensor is:

$$\sigma = 2C_1\left(\lambda^2 - \frac{1}{\lambda}\right) + 2C_2\left({\lambda_e}^2 - \frac{1}{\lambda_e}\right) \tag{7}$$

where σ is the stress for a tensile test along the direction $\vec{x}$ and λ and λ_e the global and elastic stretches along the same direction. To determine the deformation of elastic and inelastic parts, i.e. the left Cauchy Green tensor of the elastic part, it is necessary to establish an evolution equation of $\mathbf{B_e}$, which is deduced as the simplest sufficient condition to satisfy Eq.(6). As described by Huber and Tsakmakis (2000) and Petiteau *et al.* (2012), the evolution equation is

$$\dot{\mathbf{B}}_\mathbf{e} = \mathbf{L}\mathbf{B_e} + \mathbf{B_e}\mathbf{L}^T - 4\frac{C_2}{\eta}\left({\mathbf{B_e}}^2 - \frac{1}{3}I_{1Be}\mathbf{B_e}\right) \tag{8}$$

where η is a material parameter. Particularly, in uniaxial extension the expression can be written by means of the stretch of the elastic part:

$$\dot{\lambda_e} = \lambda_e\frac{\dot{\lambda}}{\lambda} - 4\frac{C_2}{3\eta}(\lambda_e^3 - 1) \tag{9}$$

2.2. Convolution Integral Model

The CIM model is an adaptation of a K-BKZ formulation (Berstein *et al.*, 1963). By using the same model as Petiteau *et al.* (2012) the stress endured by an incompressible material can be expressed as follow:

$$\sigma = -p(t)\mathbf{I} + 2g_0\mathbf{B}(t) - 2\mathbf{F}(t)\int_{-\infty}^{t} g_1\exp\left(-\frac{t-\tau}{\tau_r}\right)\frac{\partial\mathbf{C}^{-1}(\tau)}{\partial\tau}d\tau\mathbf{F}^T(t) \tag{10}$$

where g_0, g_1 are material parameters that represent the stiffness of the material and are expressed in MPa and τ_r is a material parameter that represents a relaxation time in seconds. Adapted to uniaxial extension in direction $\vec{x}$, the model can be defined as:

$$\sigma = 2g_0\left(\lambda^2(t) - \frac{1}{\lambda(t)}\right) + \int_{-\infty}^{t} 2g_1\exp\left(-\frac{t-\tau}{\tau_r}\right)\left[\frac{1}{\lambda(\tau)}\frac{\partial\lambda(t)}{\partial\tau}\left(2\frac{\lambda(t)^2}{\lambda(\tau)^2} + \frac{\lambda(t)}{\lambda(\tau)}\right)\right]d\tau \tag{11}$$

3. Homogeneization on the sphere unit

3.1. General definition

The formulations previously presented (Eq.(5) and Eq.(10)) are isotropic. To turn it into a possible anisotropic formulation it is proposed to adapt the model with a sphere unit formulation, i.e. a spatial repartition of n directions, where each direction is defined by an initial vector $\mathbf{A}^{(i)}$ transformed in a vector $\mathbf{a}^{(i)}$ after deformation by $\mathbf{a}^{(i)} = \mathbf{F}\mathbf{A}^{(i)}$, where i is the number of the direction. It is often considered that each direction corresponds to a macromolecular chain and thus each chain can endure only tension-compression. To take into account the behavior of a material according to different directions, the fourth invariant $I_4^{(i)}$ is used. It is to note that the elongation and the fourth invariant are equivalent according to the definition:

$$I_4{}^{(i)} = \mathbf{A}^{(i)}.\mathbf{C}\mathbf{A}^{(i)} = {\lambda^{(i)}}^2 \tag{12}$$

Where $\mathbf{C} = \mathbf{F}^T\mathbf{F}$ is the right Cauchy Green strain tensor. The following sections describe how to turn the models described previously into spherical models.

3.2. Application of the sphere unit to the two viscoelastic models

3.2.1. IVM

For IVM formulations, the location of the rotation in the decomposition between the elastic and the inelastic parts (cf. Eq.(5)) is still an open issue. Indeed it is often estimated that the rotation endured by the material occurs into the elastic part and not into the inelastic one. By means of this spherical formulation, the problem does not occur since each direction is only submitted to tension, that means that there is no hypothesis to formulate about the rotation in this approach. It is proposed to turn the IVM into a sphere unit formulation, thus each expression described previously has to be adapted. First, the evolution equation of the IVM is just adapted from Eq.(8) to be defined along n directions, it writes for each direction i:

$$\dot{\mathbf{B}}_\mathbf{e}^{(i)} = \mathbf{L}^{(i)}\mathbf{B_e}^{(i)} + \mathbf{B_e}^{(i)}\mathbf{L}^{T(i)} - 4\frac{C_2}{\eta}\left(\mathbf{B_e}^{(i)^2} - \frac{1}{3}I_{1Be}\mathbf{B_e}^{(i)}\right) \tag{13}$$

thus for uniaxial extension:

$$\dot{\lambda}_e^{(i)} = {\lambda_e}^{(i)}\frac{\dot{\lambda}^{(i)}}{\lambda^{(i)}} - 4\frac{C_2}{3\eta}\left({\lambda_e^{(i)}}^3 - 1\right) \tag{14}$$

by means of this expression one can obtain the value of the stress in each direction:

$$\sigma^{(i)} = 2C_1\left({\lambda^{(i)}}^2 - \frac{1}{\lambda^{(i)}}\right) + 2C_2\left({\lambda_e^{(i)}}^2 - \frac{1}{\lambda_e^{(i)}}\right) \tag{15}$$

3.2.2. CIM

To adapt the formulation of the CIM, the previous equation Eq.(11) must also be defined in n directions. Thus for the CIM, and due to the hypothesis of uniaxial extension the n directions can be described only by $\lambda^{(i)}(t)$. The stress for each direction can be deduced from the Eq.(11):

$$\sigma^{(i)} = 2g_0\left({\lambda^{(i)}}^2(t) - \frac{1}{\lambda^{(i)}(t)}\right) + \int_{-\infty}^{t} 2g_1\exp\left(-\frac{t-\tau}{\tau_r}\right)\left[\frac{1}{\lambda^{(i)}(\tau)}\frac{\partial\lambda^{(i)}(t)}{\partial\tau}\left(2\frac{{\lambda^{(i)}}^2(t)}{{\lambda^{(i)}}^2(\tau)} + \frac{\lambda^{(i)}(t)}{\lambda^{(i)}(\tau)}\right)\right]d\tau \tag{16}$$

3.2.3. Definition of the global stress

In this paper, it is proposed to use the spatial repartition of 42 directions proposed by Bazant and Oh (1986). This discretization is homogeneously spread in space and allow to describe an isotropic behavior. The choice of 42 directions is made because they well represent the space and limit also the anisotropy due to the discretization as explained by Gillibert *et al.* (2010). To obtain the total stress endured by the material, it is necessary to sum the influence of each direction by applying a weight $\omega^{(i)}$. Thus, the stress induced by the material for both models is defined as:

$$\boldsymbol{\sigma} = \sum_{i}^{42} \omega^{(i)} \sigma^{(i)} (\mathbf{a}_n^{(i)} \otimes \mathbf{a}_n^{(i)}) \tag{17}$$

where $\mathbf{a}_n^{(i)}$ is the normalized vector for each direction, i.e. $\mathbf{a}_n^{(i)} = \frac{\mathbf{a}^{(i)}}{\|\mathbf{a}^{(i)}\|}$ and $\sigma^{(i)}$ is given by Eq.(15) or Eq.(16) according to the chosen model. The spatial repartition of 42 directions used and proposed by Bazant and Oh (1986) is represented according to different plans in Fig.2. The Fig.2(a) represents the directions in the plan $(\vec{y}, \vec{z})$. It appears that each direction belong to a circle. A representation of the different circles is illustrated in the plan $(\vec{x}, \vec{z})$ in Fig.2(b).

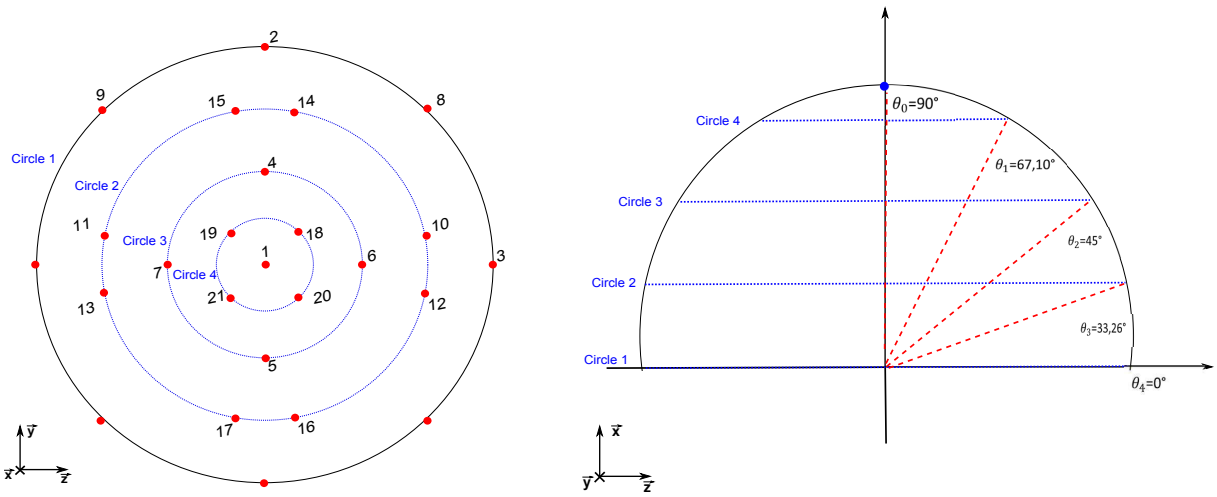

Figure 2: Representation of the 42 direction of Bazant and Oh (1986) (a) in the plan $(\vec{y}, \vec{z})$, (b) and in the plan $(\vec{x}, \vec{z})$.

3.2.4. Simulation of the sphere unit models

It is proposed in this section to compare the results for a same loading for classical and spherical formulations and for both models at several strain rates. The Fig.3(a) highlights the results obtained for two cycles tensile tests up to $\lambda = 4$ along the direction $\vec{x}$ for the IVM classical formulation (as presented in Petiteau *et al.* (2012)) and Fig.3(b) the results with the spherical formulation for the IVM. For both simulations the parameters used are identical as those used by Petiteau *et al.*

(2012): $C_1 = 1$ MPa ; $C_2 = 9$ MPa and $\eta = 1$MPa.s. It is observed that the obtained behaviors are different for the two formulations, the results of the spherical formulation provide a lower response than the classical formulation for all the different strain rates studied. But the influence of the strain rate is similar for the two formulations. In the same way it is proposed to highlight the

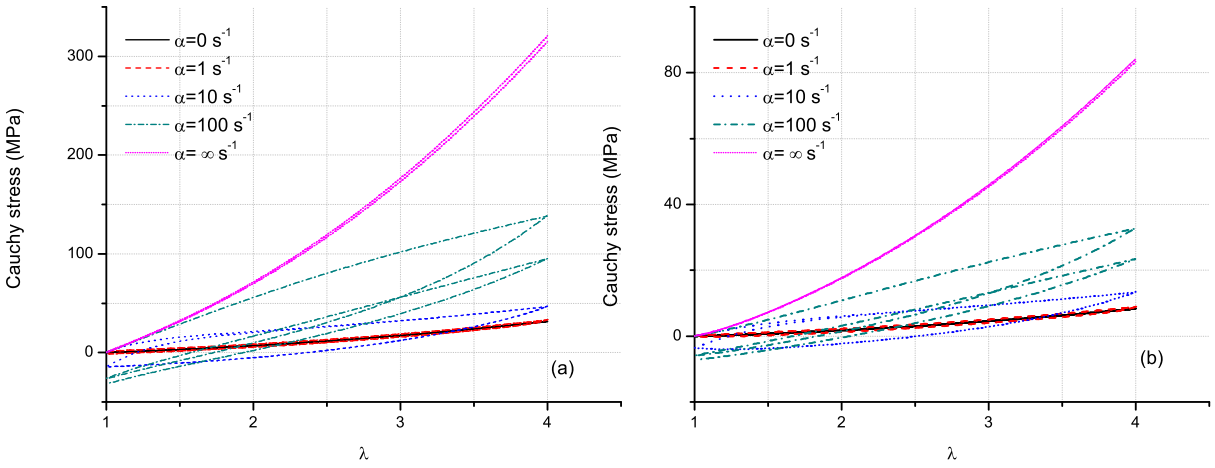

Figure 3: Stress strain curve IVM for an isotropic formulation (a) and a sphere unit formulation with 42 directions (b)

most requests directions for the spherical formulation. A weight stress tensor can be associated to each direction, i.e. $w^{(i)}\sigma^{(i)}(\mathbf{a}_n^{(i)} \otimes \mathbf{a}_n^{(i)})$, the contribution of the weight stress tensor along the tensile direction is illustrated in Fig.4 for a strain rate of $\alpha = 100$ s^{-1}. It is to note that each direction that belongs to a same circle (cf. Fig.2) presents the same mechanical behavior. Moreover, it is observed that some directions do not have any influence: directions 2-3-8-9 which belong to the circle 1 as illustrated in Fig.2. Indeed it is consistent that these directions do not present any influence since the directions of the circle 1 projected in the direction $\overrightarrow{x}$ (which matches to the tensile direction) is equal to zero. The other directions present an increasing contribution for the circles 2, 3, 4 and for the direction 1 which corresponds to the tensile direction.

It is proposed to realize the same two cycles tensile test up to $\lambda = 4$ with the classical and spherical formulations of the CIM. The obtained results are presented in Fig.5. The parameters used are identical as those used by Petiteau *et al.* (2012): $g_0 = 1$ MPa, $g_1 = 9$ MPa and $\tau_r = \frac{1}{36}$ s. As previously, both formulations do not predict the same behavior, but the influence of the strain rate is similar. Indeed the spherical formulation induced a lower stress state than the classical formulation for the same strain state at different strain rates. The stress state for each direction can be observed in Fig.6 for a strain rate of $\alpha = 100$ s^{-1} and for the same mechanical parameter. As previously, the most request direction is the direction 1 since it is the direction that corresponds to the tensile direction $\overrightarrow{x}$.

3.2.5. Comparison of the two theories with a sphere unit formulation

As proved for the classical formulation by Petiteau *et al.* (2012), it appears that the two models exhibit the same response, even if the strengthening is larger for CIM than for IVM. Furthermore, the hysteresis loop is larger for IVM than for CIM. These differences are more important at high

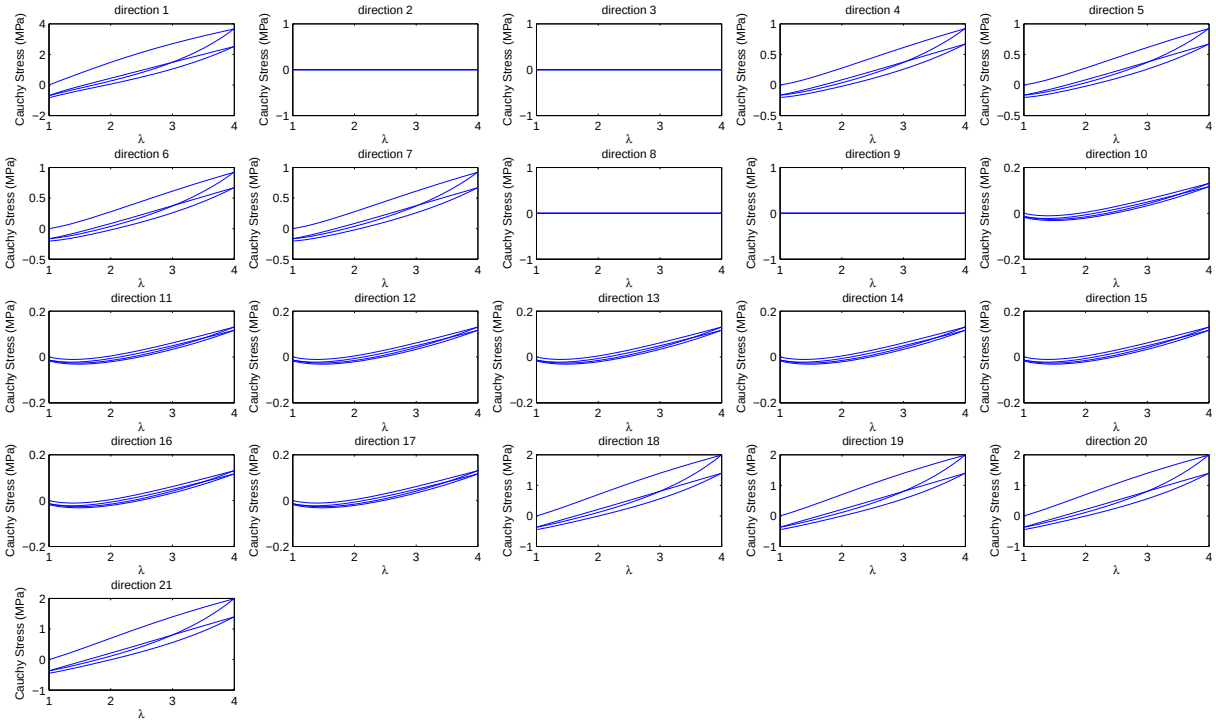

Figure 4: Stress strain curves for IVM for the 42 directions of the sphere unit model

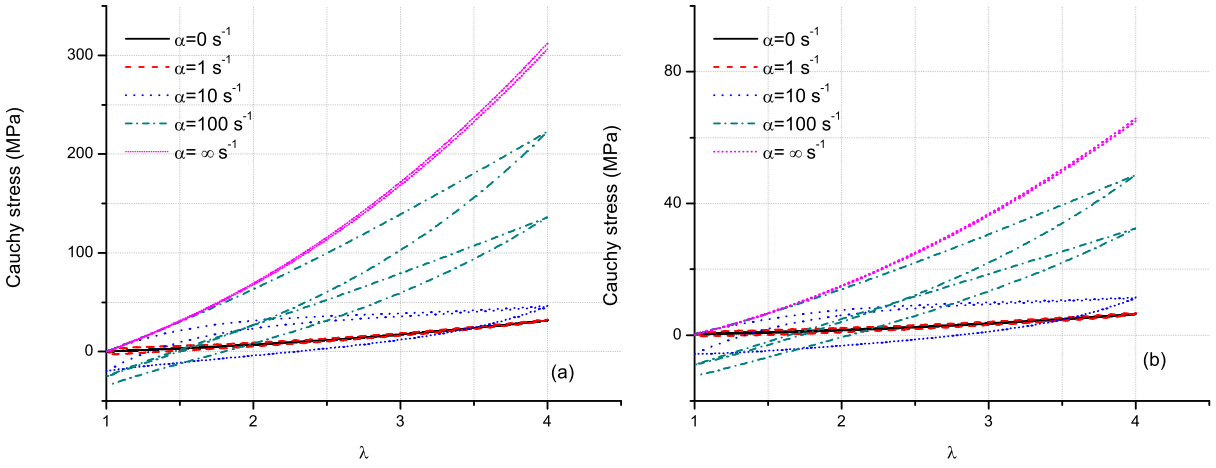

Figure 5: Stress strain curve of the CIM model for an isotropic formulation (a) and a sphere unit formulation with 42 directions (b)

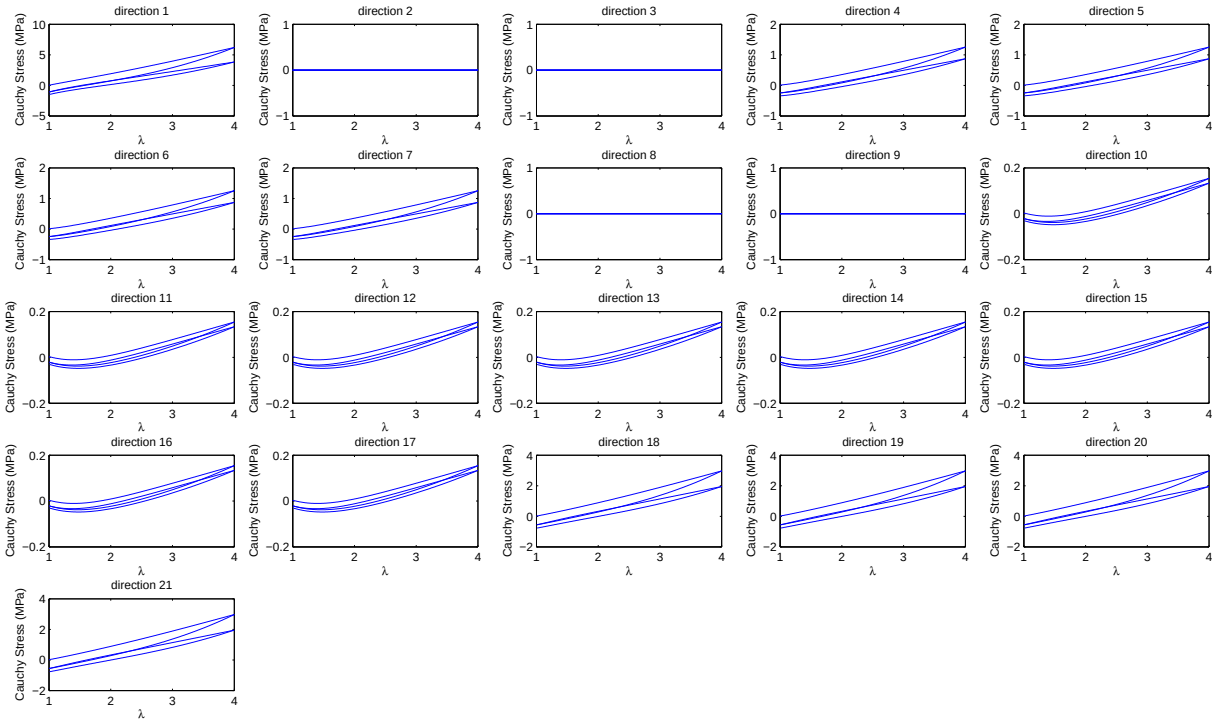

Figure 6: Stress strain curves for CIM for the 42 directions of the sphere unit model

strain rates. With the sphere unit formulation it is observed that both models exhibit also similar responses, still with some differences, as illustrated in Fig.3(b) and Fig.5(b). Indeed for all strain rates the two models present a different strengthening (larger for CIM than IVM) and hysteresis (larger for IVM than CIM). The differences are still more important for high strain rates. It is to note that the results of the sphere unit formulation are similar to the classical formulation for both models with a scale factor at each strain rates. This sphere unit formulation provides similar results as those of Miehe and Göktepe (2005); Diani *et al.* (2006) for isotropic materials. It is to note that the sphere unit formulation is based on a Neo Hookean constitutive equation but could be represented by any phenomenological constitutive equation instead of micro mechanics model based on Langevin function as proposed by Miehe and Göktepe (2005); Diani *et al.* (2006). Anyway, the spherical formulation can be adapted to any strain energy density.

4. Comparison of the classical formulations and the sphere unit formulations for different mechanical loadings

In this part, it is proposed to compare the results obtained with a classical formulation and a spherical formulation for the IVM and the CIM according to different loadings states. For each formulation and model, it is proposed to simulate a two cycles test up to $\lambda = 4$ for uniaxial (UT), planar (PT) and equibiaxial (ET) tests. The stress equations for planar and equibiaxial tests are easily deduced from Eq.(5) and Eq.(8) for the IVM and from the Eq.(10) for the CIM. The Fig.7 illustrates the results obtained for the IVM and the CIM with the classical formulation. It is observed that the three mechanical tests provide approximately the same response, the first load and

the beginning of the first unload. For the ET it is observed that the models cannot truly take into account the viscoelasticity since the tests present highly compressive stress during the unloading, these results are not consistent with the experimental observations. It is also expected to obtain a stress state more important for an equibiaxial test compare to uniaxial or planar state (Treloar, 1943; Marckmann and Verron, 2006; Boyce and Arruda, 2000). This phenomenon can be explained by the unidirectional modeling used for the classical models.
The same cyclic tensile tests were performed with the sphere unit formulation for the IVM and CIM as illustrated in Fig.8. It appears that the equibiaxial tests provide a stress state more important than the uniaxial or planar tensile tests for a same strain state with the same elementary hyperelastic models. Furthermore with the sphere unit formulation, it is observed that there is only a few compressive stress during the unloading. These results are more consistent than those obtained with the classical formulation for the both models. These results highlight that the sphere unit formulation is more adapted to describe an equibiaxial test than the classical formulation for this type of viscoelastic models for classical formulations. The uniaxial and planar tensile tests are also well described by the sphere unit formulation.

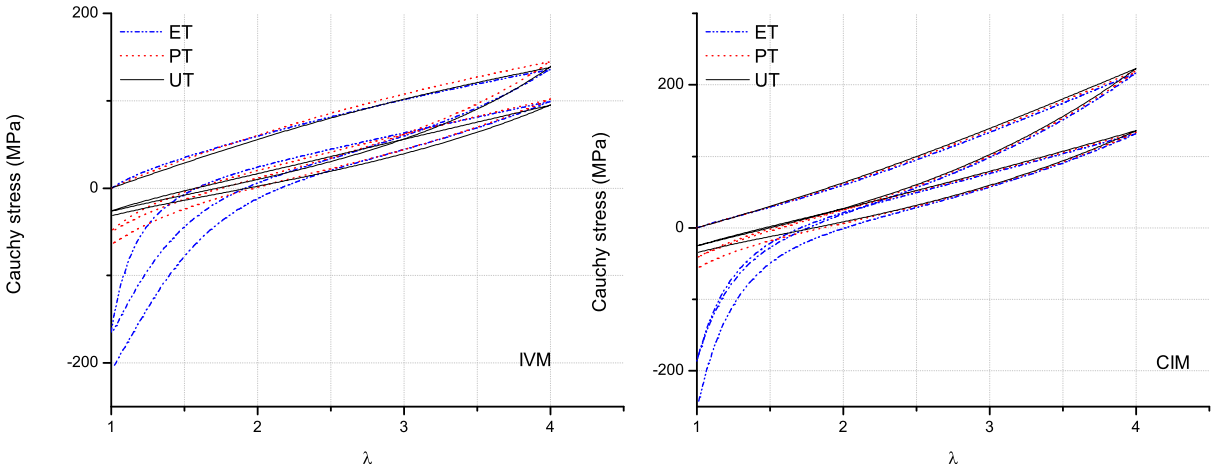

Figure 7: Stress-strain curves for uniaxial (UT), planar (PT) and equibiaxial (ET) tension for isotropic formulation with the IVM and the CIM

In conclusion, these simulations prove that simple tensorial form models cannot be easily used to represent biaxial loading, and leads to inconsistent results. At the opposite the use of spherical approach to represent three dimensional loadings is efficient even if the three dimensional homogenization is based on simple tensorial form issue from uniaxial development.

5. Extension to anisotropic viscoelasticity

By means of the spatial repartition of the directions used previously, an isotropic viscoelastic formulation was written. It is proposed now to use the sphere unit formulation to obtain an anisotropic response by a parametric study of the different directions. That means that each direction is no longer represented by the same mechanical parameter. With the sphere unit formulation, the directions are homogeneously distributed in space, a projection of this distribution was presented in Fig.2. This homogenous repartition of the directions induces a quasi isotropic behavior

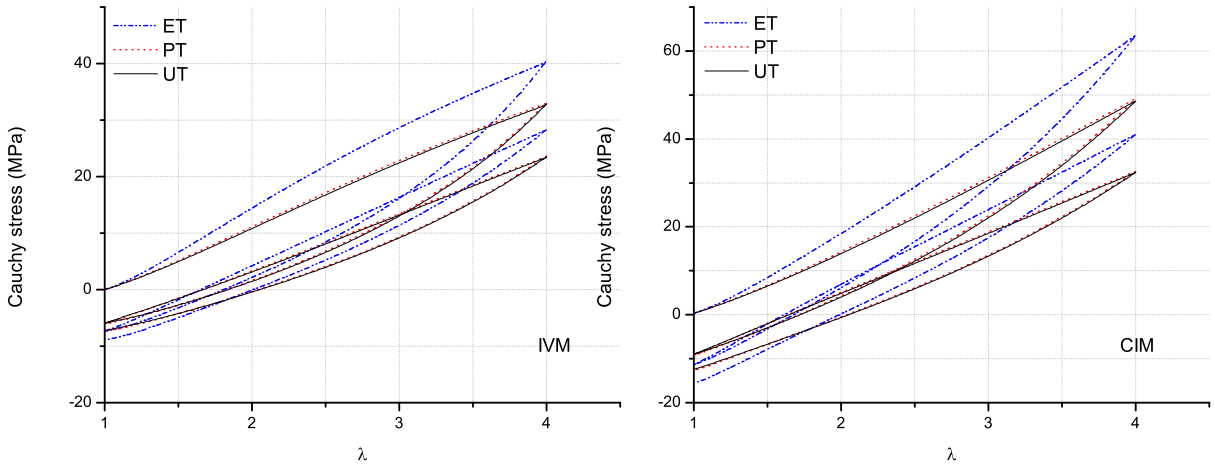

Figure 8: Stress-strain curves for uniaxial (UT), planar (PT) and equibiaxial (ET) tension for sphere unit formulation with the IVM and the CIM

(Gillibert *et al.*, 2010). Thus, the results obtained for a tensile test along the direction $\vec{x}$ or $\vec{y}$ are identical.

5.1. Variation of the viscoelastic parameter (η and τ_r)

5.1.1. Presentation

It is proposed to induce a variation of the viscoelastic parameters η for the IVM and τ_r for the CIM. The variation of the viscoelastic terms do not change the expressions of the stress described previously. Except that, it is considered that this parameter depends on the considered directions as illustrated in Fig.9. To highlight the influence of an anisotropic formulation compared to an isotropic formulation, several numerical simulations are performed:

- First, a cyclic tensile test along the direction $\vec{x}$ until a stretch of $\lambda = 4$ is performed for a sphere unit formulation where the viscoelastic term is constant in each direction: $\eta(i) = 1$ MPa.s and $\tau_r(i) = \frac{1}{36}$ s $\forall i$, these tests are denoted (**dir1 − isotropic**).

- Then the same cyclic test along $\vec{x}$ is performed for a variation of the viscoelastic term for each direction as described previously and illustrated in Fig.9: $\eta(i) = \eta_0 \cos(\theta_i)$ and $\tau_r(i) = \tau_{r0} \cos(\theta_i)$ where $\eta_0 = 1$ MPa.s and $\tau_{r0} = \frac{1}{36}$ s, these tests are denoted (**dir1 − anisotropic**).

- Finally the same cyclic tensile test, with the variation of the viscoelastic parameters ($\eta(i) = \eta_0 \cos(\theta_i)$ and $\tau_r(i) = \tau_{r0} \cos(\theta_i)$), is performed along the direction $\vec{y}$, these tests are denoted (**dir2 − anisotropic**).

These simulations are performed for both models (IVM and CIM) and the same sets of mechanical parameters defined previously are used (cf. paragraph 3.2.4). All the results are simulated for a strain rate $\alpha = 100$ s^{-1}.

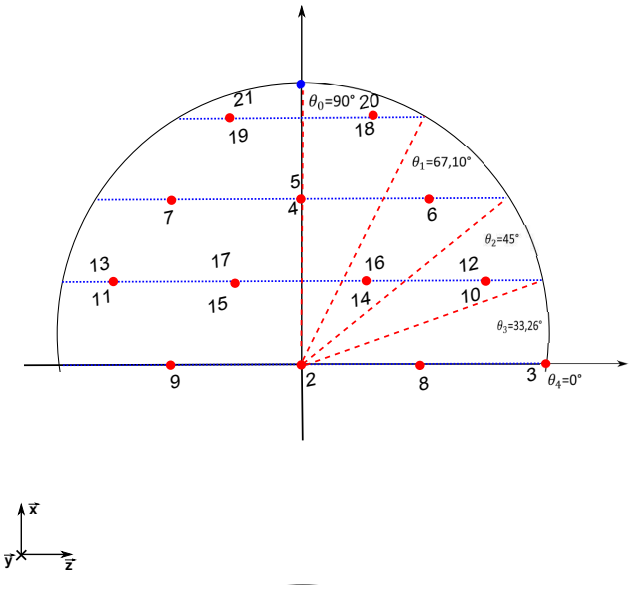

$$\eta = \eta_0 \cos(\theta_0) \qquad \tau_r = \tau_{r0} \cos(\theta_0)$$
$$\eta = \eta_0 \cos(\theta_1) \qquad \tau_r = \tau_{r0} \cos(\theta_1)$$
$$\eta = \eta_0 \cos(\theta_2) \qquad \tau_r = \tau_{r0} \cos(\theta_2)$$
$$\eta = \eta_0 \cos(\theta_3) \qquad \tau_r = \tau_{r0} \cos(\theta_3)$$
$$\eta = \eta_0 \cos(\theta_4) \qquad \tau_r = \tau_{r0} \cos(\theta_4)$$

Figure 9: Representation of the spatial distribution of Bazant and Oh directions in the plan $(\vec{y}, \vec{z})$

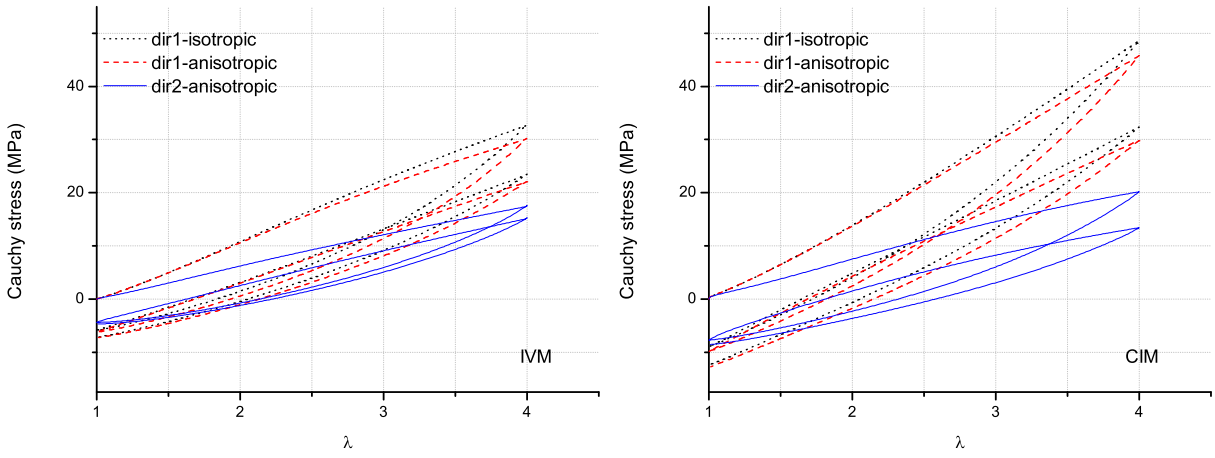

Figure 10: Variation of the viscoelastic parameter τ_r and η for the both model IVM and CIM, the other parameters are identical for a cyclic uniaxial tensile test.

5.1.2. Analysis

The results of the tests described previously for the IVM and the CIM are presented in Fig.10. It is observed that the results are similar for the CIM (variation of τ_r), and for the IVM (variation of η). Indeed the stress strain curves obtained for (**dir1 – isotropic**) and (**dir1 – anisotropic**) are very similar, the predominant direction in the spherical approach is the closest one from the loading direction. As the viscoelastic parameters were not changed in direction 1 the mechanical behavior is not so modified. At the opposite, the stress strain curve (**dir2 – anisotropic**) is very lower than the stress strain curves corresponding to a tensile test along the direction $\vec{x}$. Thus, it proves that with the spherical formulation the two models can easily represent a multidirectional anisotropic viscoelastic behavior.

5.2. Variation of the hyperelastic parameter of the inelastic part (g_1 and C_2)

5.2.1. Presentation

It is proposed for this second study to vary a second material parameter. The C_2 (IVM) or g_1 (CIM) parameters, are not the same in all directions. Thus, the variation of the parameters is expressed in the same way as previously, that means that C_2 and g_1 are now depending on the orientation of the directions in space as illustrated in Fig.11. As previously several tests are

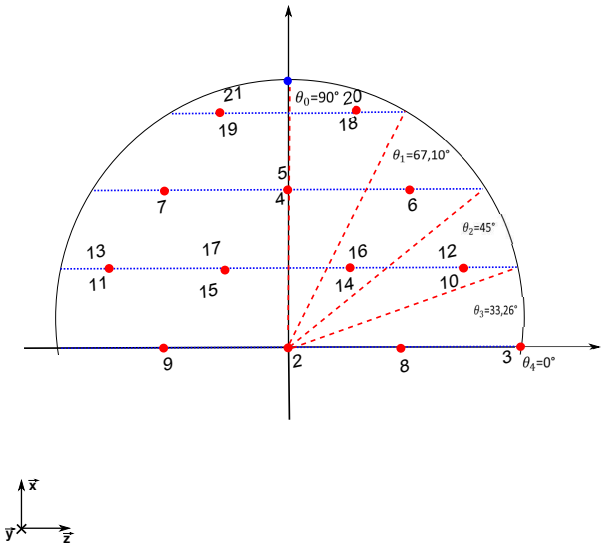

$$C_2 = C_{2-0}\cos(\theta_0) \qquad g_1 = g_{1-0}\cos(\theta_0)$$
$$C_2 = C_{2-0}\cos(\theta_1) \qquad g_1 = g_{1-0}\cos(\theta_1)$$
$$C_2 = C_{2-0}\cos(\theta_2) \qquad g_1 = g_{1-0}\cos(\theta_2)$$
$$C_2 = C_{2-0}\cos(\theta_3) \qquad g_1 = g_{1-0}\cos(\theta_3)$$
$$C_2 = C_{2-0}\cos(\theta_4) \qquad g_1 = g_{1-0}\cos(\theta_4)$$

IVM CIM

Figure 11: Representation of the spatial distribution of Bazant and Oh directions in the plan $(\vec{y}, \vec{z})$

performed:

- First a tensile test along $\vec{x}$ until a stretch of $\lambda = 4$ for a constant value of the parameters in each direction: $C_2(i) = 9$ MPa and $g_1(i) = 9$ MPa $\forall i$, these tests are denoted (**dir1 – isotropic**).

- Then the same tensile test in the direction $\vec{x}$ with varying values of the parameters: $C_2 = C_{2-0}\cos(\theta_i)$ and $g_1 = g_{1-0}\cos(\theta_i)$ where $C_{2-0} = 9$ MPa and $g_{1-0} = 9$ MPa, these tests are denoted (**dir1 – anisotropic**).

- Finally, still the same tensile test along the direction $\vec{y}$ with also varying values (**dir2 – anisotropic**) is performed.

5.2.2. Analysis

The results can be observed in Fig.12, where g_1 and C_2 are varying and the other mechanical parameters are constant, the simulations are presented for a strain rate $\alpha = 100\ \mathrm{s}^{-1}$. As previously

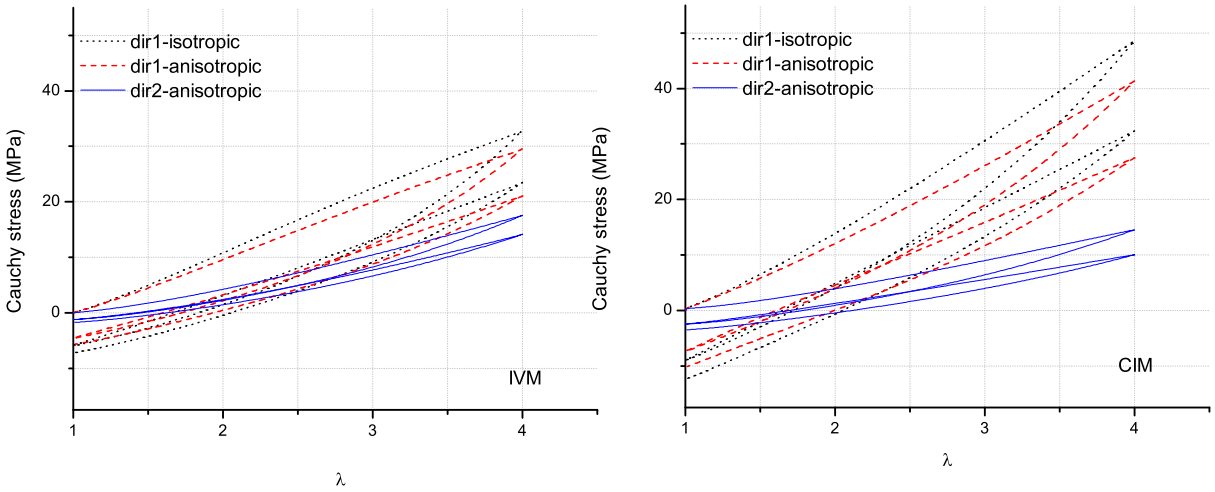

Figure 12: Variation of g_1 and C_2 for the both models IVM and CIM, the other parameters are still the same (where η and τ are constant) for a cyclic uniaxial tensile test.

it is observed that for a tensile test along the direction $\vec{x}$ the results are quite similar for the both models, even if the anisotropic spherical formulation (**dir1 – anisotropic**) provides lower results as the isotropic spherical formulation (**dir1 – isotropic**). The tensile tests along the direction $\vec{y}$ for the anisotropic spherical formulation (**dir2 – anisotropic**) present results lower than the two other stress strain curves for both models. Thus, by varying these other mechanical parameters it is also possible to obtain an anisotropic behavior for both models, and the behavior of the chain oriented in the loading direction is still predominant.

5.3. Conclusions

According to this study, it was observed that, by means of a sphere unit formulation, it is easy to obtain an anisotropic behavior. The anisotropy of a material was induced by means of the mechanical parameters. All the parameters do not induce the same anisotropic response. Thus, it is possible to turn a material anisotropic as wished. The results presented in this paragraph where performed at $\alpha = 100\mathrm{s}^{-1}$, but the conclusions are identical for other strain rates. Compared to others pre-existent models about viscoelasticity, it is to note that there is only a few proposed models in literature (Miehe and Göktepe, 2005; Diani *et al.*, 2006) to take into account a multidirectional anisotropic viscoelastic behavior. Miehe and Göktepe (2005) proposed an adaptation of its initial model to take into account anisotropic behavior and Diani *et al.* (2006) proposed a model to take into account the induced anisotropy due to the stress softening. Most of the anisotropic models are developed for soft tissues but they only present two different directions, due mainly to the fiber reinforcement in the material Peña *et al.* (2007); Taylor *et al.* (2009). The model

presented here allows to take into account the initial anisotropy of a material by the simple way of a sphere unit formulation and can thus represented a multidirectional anisotropy by means of a simple phenomenological model.

6. Viscoelasticity and Mullins effect

As explained previously the viscoelasticity is one of the non linear phenomenon associated to rubberlike materials and soft tissues. Nevertheless other phenomena as Mullins effect or permanent set are also current for this materials. It is proposed in this part to add the phenomenological stress softening model developed by Rebouah *et al.* (2013) at the CIM and IVM to take into account the Mullins effect in the previous sphere unit viscoelastic models. It is to note that any other constitutive equation for describing the Mullins effect can also be used, especially the micromechanics-based model as De Tommasi *et al.* (2006); Diani *et al.* (2006); Miehe and Göktepe (2005). The main equations are recalled here where a repartition of n initial spatial directions $\mathbf{A}^{(i)}$ is also used. The general form of the strain energy is:

$$\mathcal{W} = \mathcal{W}_{cc}(I_1) + \sum_{i=1}^{n} \omega^{(i)} \mathcal{F}^{(i)} \mathcal{W}_{cf}^{(i)}(I_4^{(i)}). \tag{18}$$

where $\mathcal{W}_{cc}$ represents the hyperelastic Neo Hookean model already used in the viscoelastic model, and $\mathcal{F}^{(i)}$ is the Mullins effect evolution function similar as the one proposed by Zuñiga and Beatty (2002) and $W_{cf}^{(i)}$ is the strain energy associated with each direction. The energy proposed by Kaliske (2000) is chosen:

$$\mathcal{W}_{cf}^{(i)} = \frac{K}{4}(I_4^{(i)} - 1)^2 \tag{19}$$

and the evolution function is:

$$\mathcal{F}^{(i)} = 1 - \eta_m \sqrt{\frac{I_{1\max} - I_1}{I_{1\max} - 3}} \left(\frac{I_{4\,\max}^{(i)} - I_4^{(i)}}{I_{4\,\max}^{(i)} - 1} \right) \left(\frac{I_{4\,\max}^{(i)}}{I_{4\,\max}} \right)^4 \tag{20}$$

where η_m is a mechanical parameter that represents the intensity of the stress softening between the first and the second loadings, and $I_{1\max}$, $I_{4\max}^{(i)}$ and $I_{4\max}$ are respectively the maximum values of I_1, ${I_4}^{(i)}$ for the direction i and ${I_4}^{(i)}$ for all directions.

6.1. IVM

The Mullins effect model was added to the viscoelastic part and thus the rheological scheme is modified as illustrated in Fig.13. The final expression of the IVM and Mullins effect model is expressed as:

$$\sigma = \sum_{i}^{42} \omega^{(i)} \left(2C_1 \left({\lambda^{(i)}}^2 - \frac{1}{\lambda^{(i)}} \right) + 2C_2 \left({\lambda_e^{(i)}}^2 - \frac{1}{\lambda_e^{(i)}} \right) + 2{\lambda^{(i)}}^2 \mathcal{F}^{(i)} {\frac{\partial W_{cf}}{\partial I_4^{(i)}}}^{(i)} \right) \mathbf{a}_n^{(i)} \otimes \mathbf{a}_n^{(i)} \tag{21}$$

It is proposed to simulate a tensile test defined by 5 cycles until $\lambda = 2$, then 5 cycles until $\lambda = 3$ and finally 5 cycles until $\lambda = 4$. A strain rate of $\alpha = 15\ \mathrm{s}^{-1}$ is imposed and the chosen parameter are: $g_0 = 1$ MPa, $g_1 = 9$ MPa, η=1 MPa.s, K=0.5 MPa and η_m=4.5. The results are illustrated in

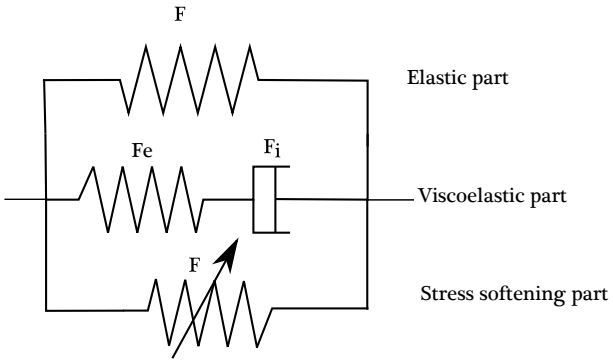

Figure 13: Representation of the viscoelastic and Mullins effect modeling

Fig.14. The behavior of the viscoelastic part (**visco**) and stress softening (**Mullins**) are represented independently and finally the sum of these two behaviors is represented (**total**). It is observed that for each cycle the Mullins effect is well taken into account and can be very well treated independently of the viscous effects. The global behavior is finally composed of hyperelasticity, viscoelasticity and stress softening.

6.2. CIM

The Mullins effect part is added to the viscoelastic part of the CIM in the same way as described for the IVM. The evolution function, and the strain energy are the same. Thus, the following expression of the stress is obtained:

$$\sigma = \sum_{i}^{42} \omega^{(i)} \left([2g_0({\lambda^{(i)}}^2(t) - \frac{1}{\lambda^{(i)}(t)})] + \int_{-\infty}^{t} 2g_1 \exp\left(-\frac{t-\tau}{\tau_r}\right) \left[\frac{1}{\lambda^{(i)}(\tau)} \frac{\partial \lambda^{(i)}(t)}{\partial \tau} \left(2\frac{{\lambda^{(i)}}^2(t)}{{\lambda^{(i)}}^2(\tau)} + \frac{\lambda^{(i)}(t)}{\lambda^{(i)}(\tau)} \right) \right] d\tau \right.$$
$$\left. + 2{\lambda^{(i)}}^2 \mathcal{F}^{(i)} \frac{\partial W_{cf}}{\partial I_4^{(i)}}^{(i)} \right) \mathbf{a}_n^{(i)} \otimes \mathbf{a}_n^{(i)} \quad (22)$$

It is also proposed to simulate the same test as the one described in paragraph 6.1. The results are obtained for a strain rate of $\alpha = 15$ s^{-1} and the material parameters are: $g_0 = 1$ MPa, $g_1 = 9$ MPa, $\tau_r = \frac{1}{36}$ s, K=0.5 MPa and η_m=4.5. The results are illustrated in Fig.15. As for the IVM it is observed that for cycles until a same strain state that the Mullins effect is well described and can be also very well treated independently as the viscous effects.

7. Conclusion

This paper has presented first an extension of Petiteau *et al.* (2012) study by proposing an adaptation of classical viscoelastic model to spherical approaches to realize a three directional homogenization in an incompressible framework. This formulation can be adapted to rubber like materials and soft tissues. Two classical models of viscoelasticity (IVM and CIM) were written by means of a spherical formulation and compared to a classical formulation. It appears that, if a homogeneous repartition of directions in space is used (isotropic behavior), the sphere unit model allows to describe better different loadings state (uniaxial, planar and equibiaxial tension) than a

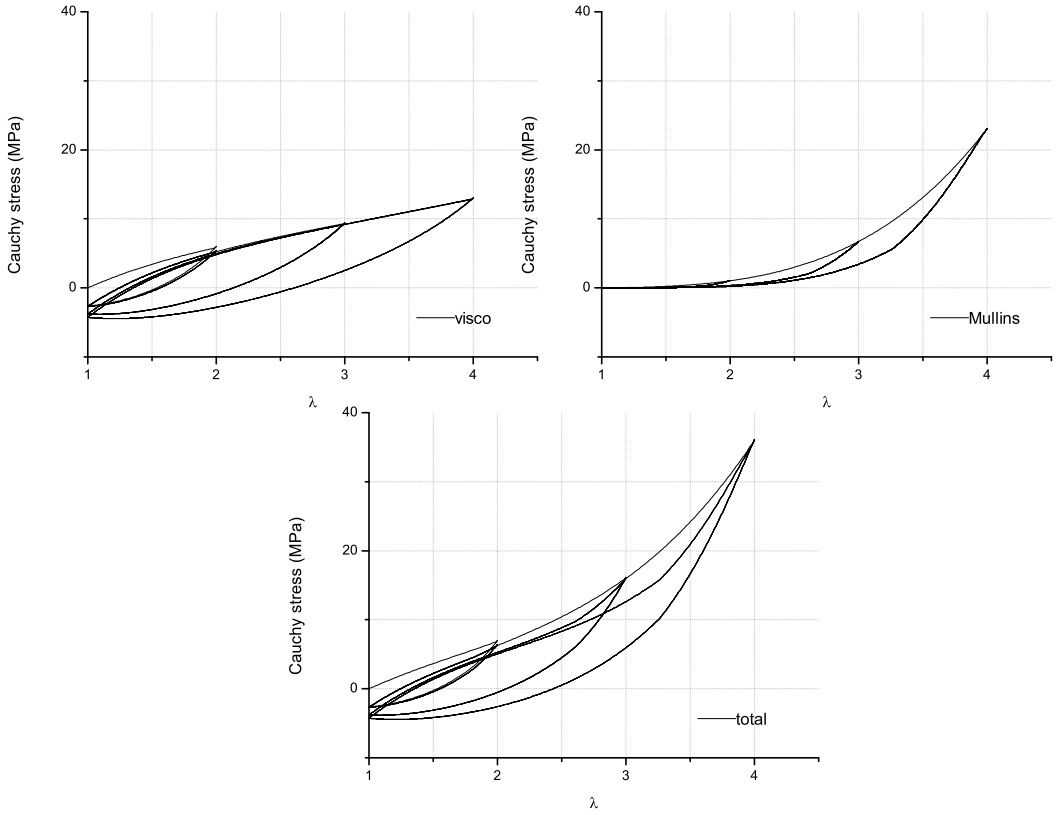

Figure 14: Simulation of 15 cycles with the IVM sphere unit model coupled with the Rebouah *et al.* (2013) stress softening model

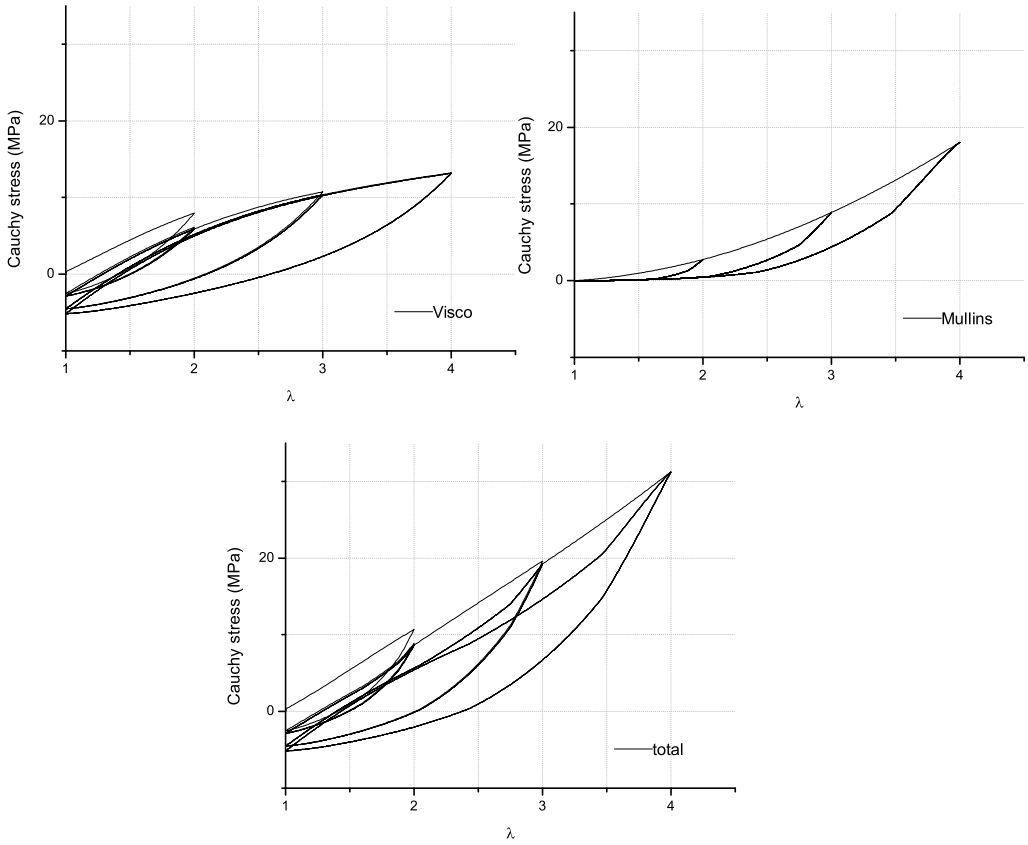

Figure 15: Simulation of 15 cycles with the CIM sphere unit model coupled with the Rebouah *et al.* (2013) stress softening model

classical formulation by correctly describing the equibiaxial extension. This permits to use these simple constitutive equations in a tridimensional framework and to be able to simulate any loading state even with simple constitutive equations.
Then, the sphere unit formulation was used to induce an initial anisotropy by imposing different mechanical parameters in each direction. It was observed that an anisotropic behavior could be easily created in this way, simply by a parameter variation along the directions. Finally, a stress softening model was added to the spherical formulation to also take into account the Mullins effect.

References

Bazant, Z. P. and Oh, B. H. (1986). Efficient numerical integration on the surface of a sphere. *Z. Angew. Math. Mech.*, **66**, 37–49.

Bergstrom, J. S. and Boyce, M. C. (1998). Constitutive modeling of the large strain time dependant behavior of elastomers. *J.Mech. Phys. Solids*, **46**(5), 931–954.

Berstein, B., Kearsley, E. A., and Zapas, L. J. (1963). A study of stress relaxation with finite strain. *Trans. Soc. Rheol.*, **7**, 391–410.

Beatty, M. F. and Krishnaswamy, S. (2000). A theory of stress-softening in incompressible isotropic materials. *J. Mech. Phys. Solids*, **48**, 1931–1965.

Boyce, M. C. and Arruda, E. M. (2000). Constitutive models of rubber elasticity: a review. *Rubber Chem. Technol.*, **73**, 504–523.

Christensen, R. (1982). *Theory of Viscoelasticity: An Introduction*. Elsevier Science.

Christensen, R. M. (1980). A nonlinear theory of viscoelasticity for application to elastomers. *J. Appl. Mech.*, **47**(4), 762–768.

Coleman, B. D. and Noll, W. (1961). Foundations of linear viscoelasticity. *Rev. Mod. Phys.*, **33**, 239–249.

Coleman, B. D. and Noll, W. (1963). The thermodynamics of elastic materials with heat conduction and viscosity *Arch. Ration. Mech. Anal.*, **13**, 167–178.

De Tommasi, D., Puglisi, G., and Saccomandi, G. (2006). A micromechanics-based model for the Mullins effect. *J. Rheol.*, **50**(4), 495–512.

De Tommasi, D., Marzano, S., Puglisi, G., and Saccomandi, G. (2010). Localization and stability in damageable amorphous solids. *Continuum Mech. Therm.*, **22**(1), 47–62.

Diani, J., Brieu, M., and Vacherand, J. M. (2006). A damage directional constitutive model for the Mullins effect with permanent set and induced anisotropy. *Eur. J. Mech. A/Solids*, **25**, 483–496.

Diani, J., Brieu, M., and Gilormini, P. (2006). Observation and modeling of the anisotropic visco-hyperelastic behavior of a rubberlike material. *Int. J. Solids Struct.*, **43**, 3044–3056.

Dorfmann, A. and Ogden, R. W. (2004). A constitutive model for the Mullins effect with permanent set in particule-reinforced rubber. *Int. J. Solids Struct.*, **41**, 1855–1878.

Fung, Y. C. (1993). *Biomechanics, Mechanical properties of living tissues*. Springer, New York, 2nd edition edition.

Gillibert, J., Brieu, M., and Diani, J. (2010). Anisotropy of direction-based constitutive models for rubber-like materials. *Int. J. Solids Struct.*, **47**(5), 640 – 646.

Govindjee, S. and Simo, J. C. (1992). Mullins' effect and the strain amplitude dependence of the storage modulus. *Int. J. Solids. Struct.*, **29**(14-15), 1737–1751.

Govindjee, S. and Simo, J. C. (1991). A micro-mechanically continuum damage model for carbon black filled rubbers incorporating Mullins' effect. *J. Mech. Phys. Solids*, **39**(1), 87–112.

Govindjee, S. and Simo, J. C. (1992b). Transition from micro-mechanics to computationally efficient phenomenology:carbon black filled rubbers incorporating Mullins' effect. *J. Mech. Phys. Solids*, **40**, 213–233.

Green, A. and Rivlin, R. (1957). The mechanics of non-linear materials with memory: Part I. *Arch. Ration. Mech. Anal.*, **1**, 1–21.

Green, M. S. and Tobolsky, A. V. (1946). A new approach for the theory of relaxing polymeric media. *J. Chem. Phys.*, **14**, 87–112.

Holzapfel, G. A. and Simo, J. C. (1996). A new viscoelastic constitutive model for continuous media at finite thermomechanical changes. *Int. J. Solids Struct.*, **33**, 3019–3034.

Huber, A. and Tsakmakis, C. (2000). Finite deformation viscoelasticity laws. *Mech. Mater.*, **32**, 1–18.

Kaliske, M. (2000). A formulation of elasticity and viscoelasticity for fibre reinforced material at small and finite strains. *Comput. Methods Appl. Mech. Engrg*, **185**, 225–243.

Kaliske, M. and Rothert, H. (1998). Constitutive approach to rate independent properties of filled elastomers. *Int. J. Solids. Struct.*, **35**(17), 2057–2071.

Limbert, G., Taylor, M., and Middleton, J. (2004). Three-dimensional finite element modelling of the human ACL: simulation of passive knee flexion with a stressed and stress-free ACL. *J. Biomech.*, **37**, 1723–1731.

Lion, A. (1996). A constitutive model for carbon black filled rubber: Experimental investigations and mathematical representation. *Continuum Mech. Therm.*, **8**, 153–169.

Lubliner, J. (1985). A model of rubber viscoelasticity. *Mech. Res. Comm.*, **12**, 93–99.

Marckmann, G. and Verron, E. (2006). Comparison of hyperelastic models for rubber-like materials. *Rubber Chem. Technol.*, **79**, 835–858.

Miehe, C. and Göktepe, S. (2005). A micro-macro approach to rubber-like materials. Part II: The micro-sphere model of finite rubber viscoelasticity. *J. Mech. Phys. Solids*, **53**, 2231–2258.

Miller, K. (2000). Constitutive modeling of abdominal organs. *J. Biomech.*, **33**, 367–373.

Miller, K. and Chinzei, K. (1997). Constitutive modelling of brain tissue: Experiment and theory. *J. Biomech.*, **30**(1112), 1115 – 1121.

Mullins, L. (1969). Softening of rubber by deformation. *Rubber Chem. Technol.*, **42**, 339–362.

Natali, A. N., Carniel, E. L., and Gregersen, H. (2009). Biomechanical behaviour of oesophageal tissues: Material and structural configuration, experimental data and constitutive analysis. *Med. Eng. & Phys.*, **31**, 1056–1062.

Ogden, R. W. (1972). Large deformation isotropic elasticity - on the correlation of theory and experiment for incompressible rubber like solids. *Proc. R. Soc. Lond. A*, **326**, 565–584.

Peña, E., Peña, J. A., and Doblaré, M. (2009). On the Mullins effect and hysteresis of fibered biological materials: A comparison between continuous and discontinuous damage models. *Int. J. Solids Struct.*, **46**, 17271735.

Peña, E., Calvo, B., Martinez, M. A., and Doblaré, M. (2007). An anisotropic visco-hyperelastic model for ligaments at finite strains. Formulation and computational aspects. *Int. J. Solids Struct.*, **44**, 760–778.

Peña, E., Martins, P., Mascarenhas, T., Natal Jorge, R. M., Ferreira, A., Doblaré, M., and Calvo, B. (2011). Mechanical characterization of the softening behavior of human vaginal tissue. *J. Mech. Beh. Biomed. Mater.*, **4**, 275–283.

Petiteau, J.-C., Verron, E., Othman, R., Sourne, H., Sigrist, J.-F., and Barras, G. (2012). Large strain rate-dependent response of elastomers at different strain rates: convolution integral vs. internal variable formulations. *Mech Time-Dep .Mat.*, pages 1–19.

Pioletti, D. P. and Rakotomanana, L. R. (2000). Non-linear viscoelastic laws for soft biological tissues. *Eur. J. Mech. A. Solids*, **19**(5), 749 – 759.

Rajagopal, K. R. and Wineman, A. S. (1992). A constitutive equation for nonlinear solids which undergo deformation inducedby microstructural changes. *Int. J. Plast.*, **8**, 385–395.

Rebouah, M., Machado, G., Chagnon, G., and Favier, D. (2013). Anisotropic Mullins stress softening of a deformed silicone holey plate. *Mech. Res. Commun.*, **49**, 36 – 43.

Reese, S. and Wriggers, P. (1997). Material instabilities of an incompressible elastic cube under triaxial tension. *Int. J. Solids Struct.*, **34**(26), 3433–3454.

Sarva, S. S., Deschanel, S., Boyce, M. C., and Chen, W. (2007). Stress strain behavior of a polyurea and a polyurethane from low to high strain rates. *Polymer*, **48**(8), 2208 – 2213.

Simo, J. C. (1987). On a fully three-dimensional finite-strain viscoelastic damage model: formulation and computational aspects. *Comp. Meth. Appl. Mech. Engng*, **60**, 153–173.

Taylor, Z., Comas, O., Cheng, M., Passenger, J., Hawkes, D., Atkinson, D., and Ourselin, S. (2009). On modelling of anisotropic viscoelasticity for soft tissue simulation: Numerical solution and GPU execution. *Med. Image Anal.*, **13**, 234 – 244.

Treloar, L. R. G. (1943). The elasticity of a network of long chain molecules (I and II). *Trans. Faraday Soc.*, **39**, 36–64 ; 241–246.

Vande Geest, J. P., Sacks, M. S., and Vorp, D. A. (2006). The effects of aneurysm on the biaxial mechanical behavior of human abdominal aorta. *J. Biomech.*, **39**, 1324–1334.

Wineman, A. S. and Rajagopal, K. R. (2000). Mechanical response of polymers. An introduction. *Cambridge University Press, Cambridge*.

Yi, J., Boyce, M. C., Lee, G. F., and Balizer, E. (2006). Large deformation rate-dependent stress-strain behavior of polyurea and polyurethanes. *Polymer*, **47**, 319–329.

Zapas, L. and Craft, T. (1965). Correlation of large longitudinal deformations with different strain histories. *Res. Natl. Bur. Stand*, **69A**, 541–546.

Zuñiga, A. E. and Beatty, M. F. (2002). Constitutive equations for amended non-gaussian network models of rubber elasticity. *Int. J. Eng. Sci.*, **40**, 2265–2294.